Boosting the Peroxidase-Like Activity of Nanostructured Nickel by Inducing Its 3+ Oxidation State in $LaNiO_3$ Perovskite and Its Application for Biomedical Assays

Xiaoyu Wang,[1] Wen Cao,[1] Li Qin,[1] Tingsheng Lin,[2] Wei Chen,[2] Shichao Lin,[1] Jia Yao,[1] Xiaozhi Zhao,[2] Min Zhou,[1] Cheng Hang,[3] and Hui Wei[1,4,*]

[1]Department of Biomedical Engineering, College of Engineering and Applied Sciences, Collaborative Innovation Center of Chemistry for Life Sciences, Nanjing National Laboratory of Microstructures, Nanjing University, Nanjing, Jiangsu, 210093, China;

[2]Department of Urology, Nanjing Drum Tower Hospital, the Affiliated Hospital of Nanjing University Medical School, Nanjing, Jiangsu, 210008, China.

[3]State Key Laboratory of Coordination Chemistry, School of Chemistry and Chemical Engineering, Nanjing University, Nanjing 210093, China.

[4]State Key Laboratory of Analytical Chemistry for Life Science, School of Chemistry and Chemical Engineering, Nanjing University, Nanjing 210093, China.

Email: weihui@nju.edu.cn; Fax: +86-25-83594648; Tel: +86-25-83593272; Web: http://weilab.nju.edu.cn.

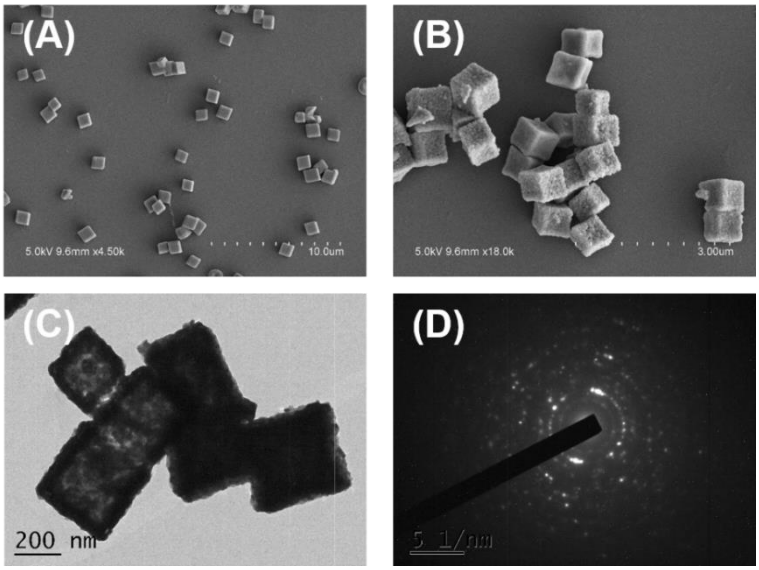

Figure S1. Representative SEM images of (A) the obtained nanocube-like precursors, and (B) the porous $LaNiO_3$ nanocubes after annealing the precursors. (C) Representative TEM image of the porous $LaNiO_3$ nanocubes. (D) Diffraction pattern of the porous $LaNiO_3$ nanocubes.

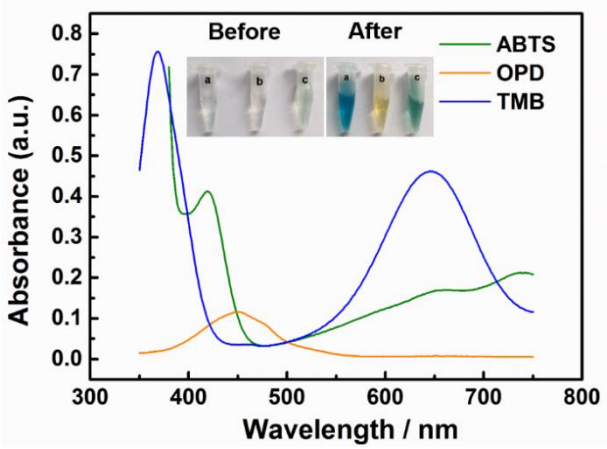

Figure S2. The absorption spectra of various peroxidase substrates catalytcially oxidized by the porous $LaNiO_3$ nanocubes. Inset: corresponding images showing the visual color changes of (a) TMB, (b) OPD, and (c) ABTS before and after the porous $LaNiO_3$ nanocubes catalyzed oxidation.

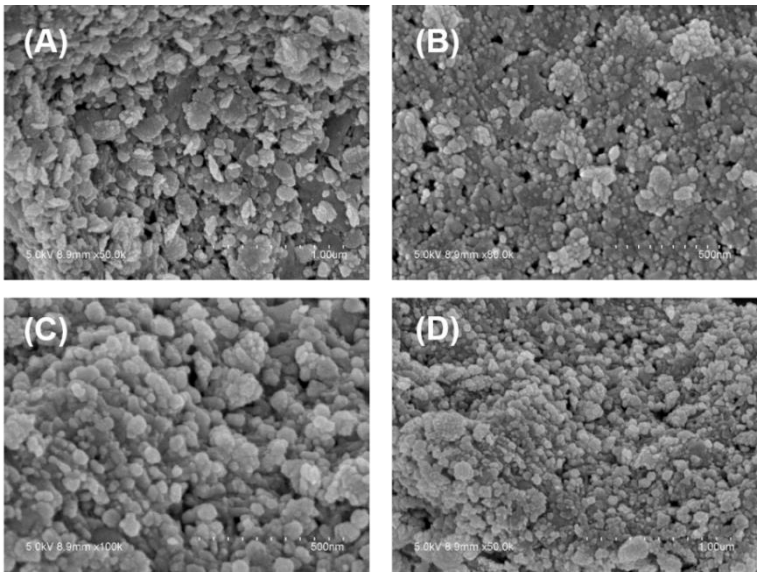

Figure S3. Representative SEM images of $LaNiO_3$-SG.

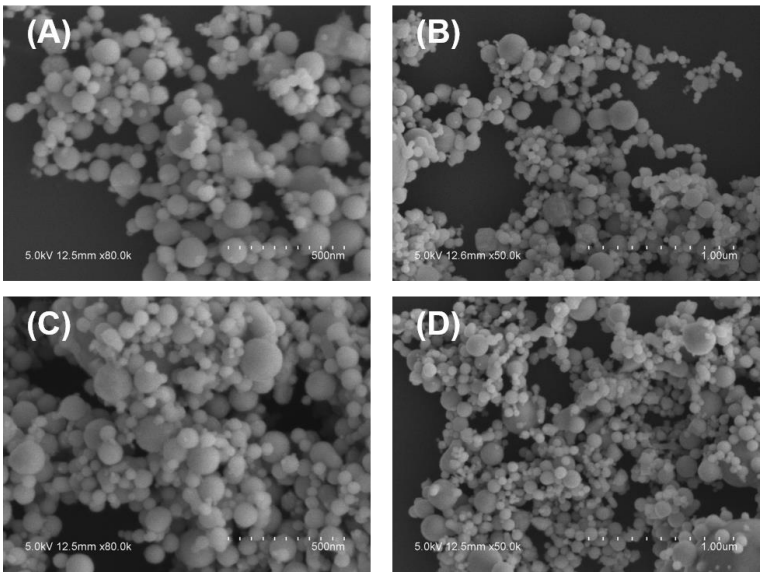

Figure S4. Representative SEM images of Ni nanoparticles.

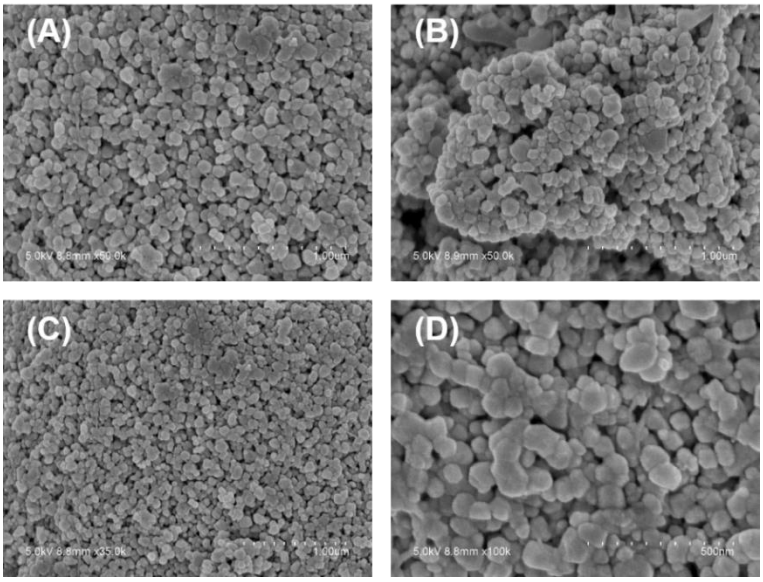

Figure S5. Representative SEM images of NiO.

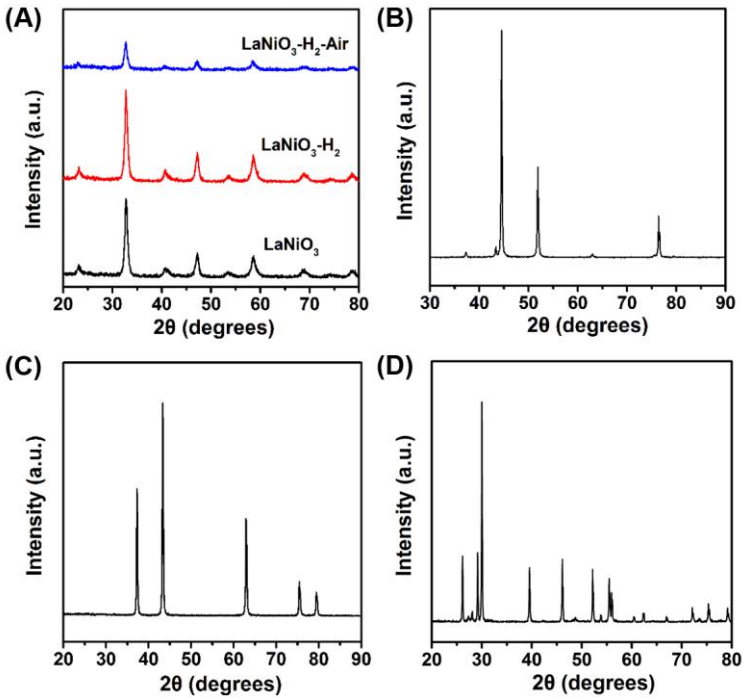

Figure S6. Powder X-ray diffraction patterns of (A) $LaNiO_3$, $LaNiO_3$-H_2, and $LaNiO_3$-H_2-Air; (B) Ni nanoparticles; (C) NiO; (D) La_2O_3.

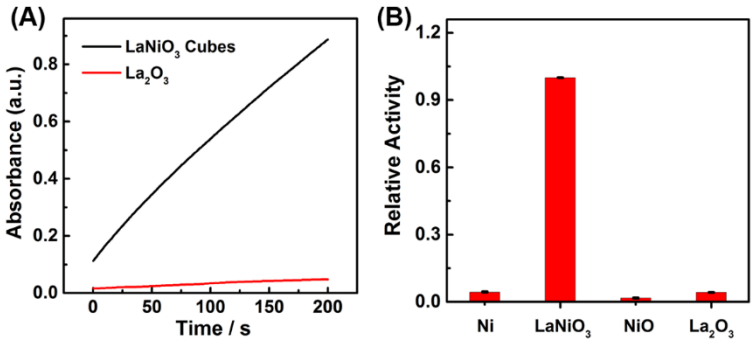

Figure S7. (A) Kinetic curves of A_{652} for monitoring the catalytic oxidation of 1 mM TMB with 40 mM H_2O_2 in the presence of 10 μg/mL of $LaNiO_3$ and La_2O_3. (B) Comparison of the peroxidase mimicking activities of Ni, $LaNiO_3$, NiO, and La_2O_3.

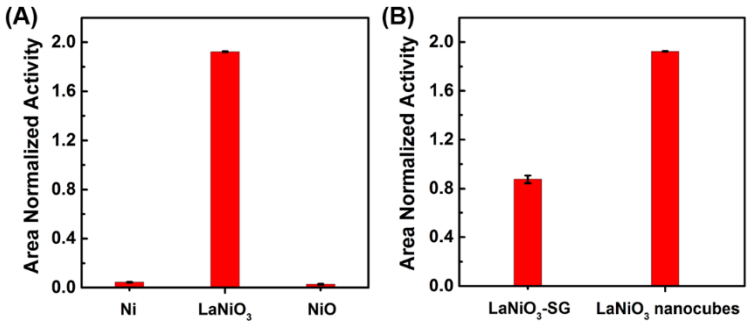

Figure S8. Comparison of the surface area normalized peroxidase mimicking activities of (A) Ni, $LaNiO_3$, and NiO; (B) $LaNiO_3$-SG and $LaNiO_3$ nanocubes.

As shown in Figure S8, the surface area normalized peroxidase-like activities of Ni-based nanomaterials were investigated to exclude the effect of surface area on the catalytic activity. As shown in Figure S8A, the surface area normalized results also showed that the oxidation state of nickel atom was very important for the peroxidase-like activity of Ni-based nanomaterials. The Ni^{3+} was the optimal oxidation state for Ni-based nanomaterials with peroxidase-like activities. As shown in Figure S8B, the $LaNiO_3$ nanocubes showed a higher surface area normalized activity than $LaNiO_3$-SG, suggesting that the effect of morphology on the peroxidase-like activity of nanomaterials. In conclusion, the results obtained from the surface area normalized activity was well agreed with those obtained from mass normalized activity.

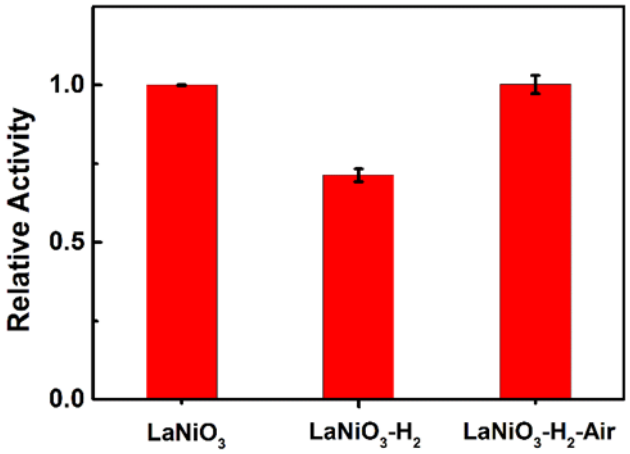

Figure S9. Comparison of the peroxidase mimicking activities of $LaNiO_3$, $LaNiO_3$-H_2, and $LaNiO_3$-H_2-Air.

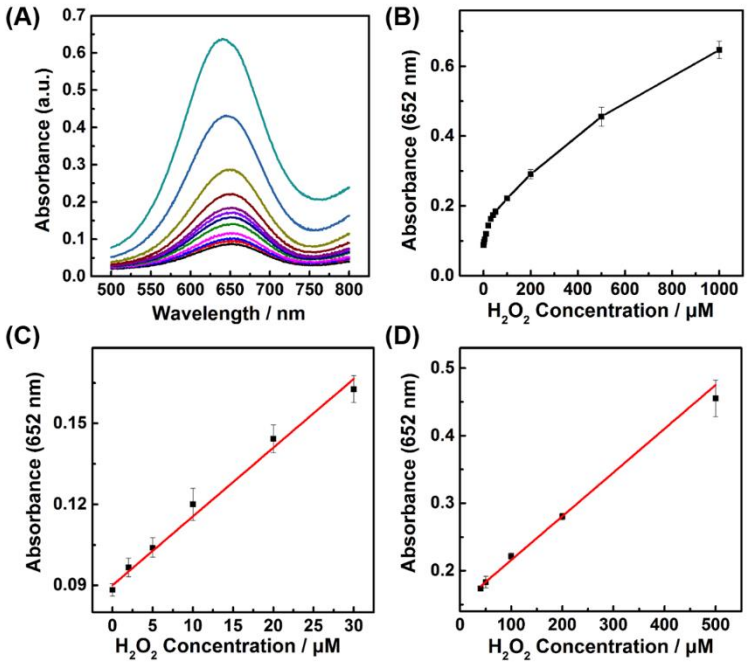

Figure S10. (A) Typical absorption spectra of TMB in the presence of different concentrations of H_2O_2. (B) Dependence of A_{652} for monitoring the catalytic oxidation of TMB on the concentration of H_2O_2 from 2 μM to 1 mM. (C, D) The linear calibration plots between the concentration of H_2O_2 and the absorbance at 652 nm.

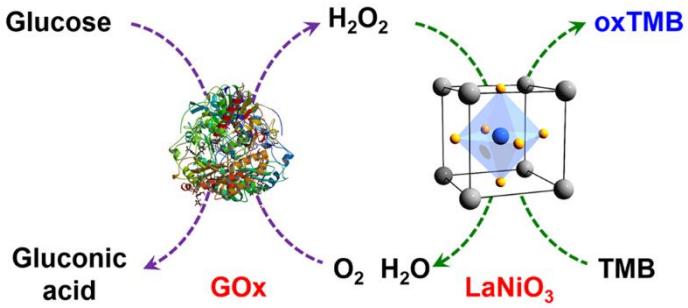

Figure S11. $LaNiO_3$ nanocubes as peroxidase mimic for colorimetric sensing of glucose by coupling with glucose oxidase (GOx).

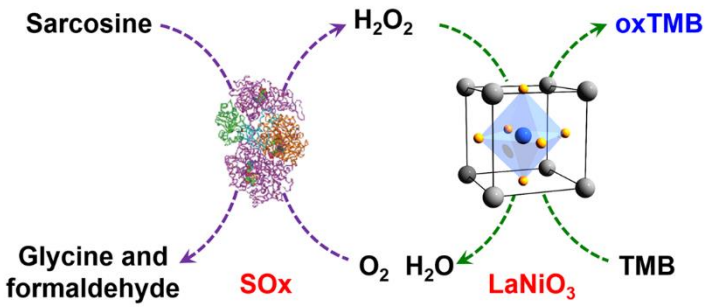

Figure S12. $LaNiO_3$ nanocubes as peroxidase mimic for colorimetric sensing of sarcosine by coupling with sarcosine oxidase (SOx).

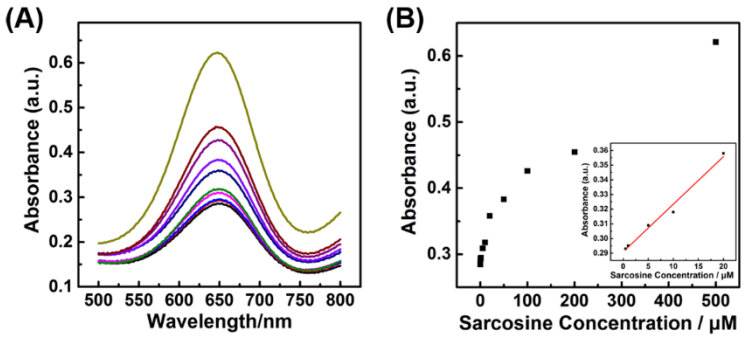

Figure S13. (A) Typical absorption spectra of TMB in the presence of different concentrations of sarcosine. (B) Dependence of A_{652} for monitoring the catalytic oxidation of TMB on the concentration of sarcosine from 0.5 μM to 500 μM. The inset shows the linear calibration plot between the concentration of sacorsine and the absorbance at 652 nm.

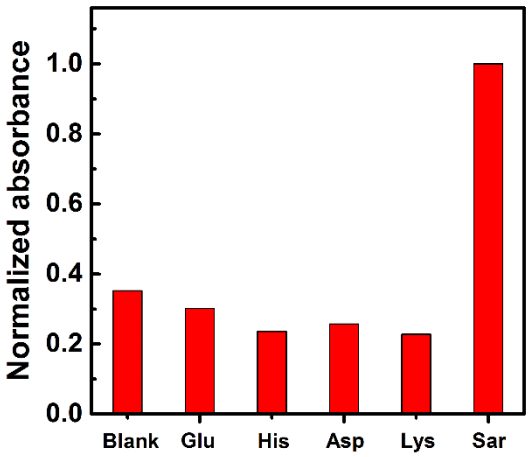

Figure S14. Selective detection of sarcosine with the porous $LaNiO_3$ nanocubes. Absorbance of TMB at 652 nm in the absence and presence of 5 mM glutamic acid (Glu), 5mM histidine (His), 5 mM aspartic acid (Asp), 5 mM lysine (Lys) and 1 mM sarcosine (Sar).

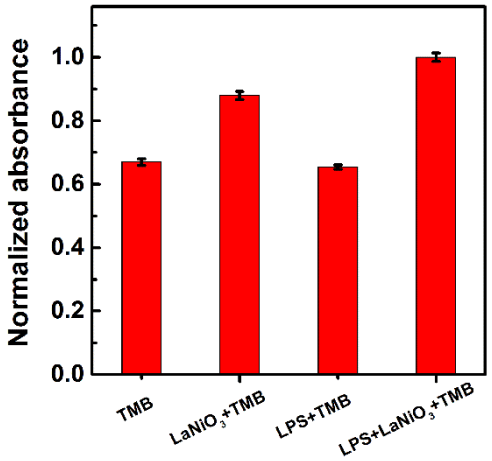

Figure S15. Colorimetric detection of *in-situ* generated H_2O_2 in Hela cells with $LaNiO_3$ nanocubes.

To detect H_2O_2 in cells, lipopolysaccharides (LPS) were used to stimulate the cells to generate H_2O_2. As shown in Figure S15, the cells with $LaNiO_3$ and TMB in the presence of LPS showed the highest colorimetric signals.

Table S1. Comparison of the kinetic parameters between porous $LaNiO_3$ nanocubes and HRP as well as other reported nanozymes

Catalyst	Substrate	K_m (mM)	V_{max} (Ms^{-1})	Ref.
$LaNiO_3$	TMB	0.105	3.62×10^{-7}	This work
$LaNiO_3$	H_2O_2	90.05	2.6×10^{-6}	This work
Pd-Ir cubes	TMB	0.13	6.5×10^{-8}	[1]
Pd-Ir cubes	H_2O_2	340	5.1×10^{-8}	[1]
GO-COOH	TMB	0.0237	3.45×10^{-8}	[2]
GO-COOH	H_2O_2	3.99	3.85×10^{-8}	[2]
Fe_3O_4	TMB	0.098	3.44×10^{-8}	[3]
Fe_3O_4	H_2O_2	154	9.78×10^{-8}	[3]
HRP	TMB	0.434	10×10^{-8}	[3]
HRP	H_2O_2	3.7	8.71×10^{-8}	[3]

K_m is the Michaelis constant, V_{max} is the maximal reaction velocity, Ref. is the abbreviation of References.

Table S2. BET surface area of the Ni-based nanomaterials studied in this work

Ni-based nanomaterials	BET surface area (m^2/g)	Normalized BET surface area
$LaNiO_3$ nanocubes	3.11	0.52
$LaNiO_3$-SG	3.79	0.63
NiO	3.65	0.61
Ni	5.93	1

Table S3. Detection of glucose in human serum samples

Serum samples	Proposed method (mM, n=3)	Glucose meter (mM)
1	10.08±1.35	11.05
2	5.71±0.92	6.00
3	10.78±1.51	12.27
4	4.31±0.89	5.05

References

1. Xia XH, Zhang JT, Lu N, Kim MJ, Ghale K, Xu Y, et al. Pd-Ir Core-Shell Nanocubes: A Type of Highly Efficient and Versatile Peroxidase Mimic. ACS Nano. 2015; 9: 9994-10004.

2. Song Y, Qu K, Zhao C, Ren J, Qu X. Graphene Oxide: Intrinsic Peroxidase Catalytic Activity and Its Application to Glucose Detection. Adv Mater. 2010; 22: 2206-2210.

3. Gao LZ, Zhuang J, Nie L, Zhang JB, Zhang Y, Gu N, et al. Intrinsic peroxidase-like activity of ferromagnetic nanoparticles. Nat Nanotechnol. 2007; 2: 577-583.